A peer-reviewed version of this preprint was published in PeerJ on 3 May 2016.

Tang Y, Luo B, Deng Z, Wang B, Liu F, Li J, Shi W, Xie H, Hu X, Li J. 2016. Mitochondrial aerobic respiration is activated during hair follicle stem cell differentiation, and its dysfunction retards hair regeneration. PeerJ 4:e1821 https://doi.org/10.7717/peerj.1821

Mitochondrial aerobic respiration is activated during hair follicle stem cells differentiation and its dysfunction retards hair regeneration

Yan Tang, Binping Luo, Zhili Deng, Ben Wang, Fangfen L Liu, Jinmao Li, Wei Shi, Hongfu Xie, Ji Li

Background. Emerging researches revealed the essential role of mitochondria in regulating stem/progenitor cell differentiation of neural progenitor cells, mesenchymal stem cells and other stem cells through reactive oxygen species (ROS), Notch or other signaling pathway. And inhibition of mitochondrial synthesis protein resulted in extension of hair loss upon injury. However, alteration of mitochondrial morphology and metabolic function during hair follicle stem cells (HFSCs) differentiation and how it affects hair regeneration has not been elaborated. **Methods.** We compared the difference between telogen bulge cells and anagen matrix cells in mitochondrial morphology and activity. Expression levels of mitochondrial ROS and superoxide dismutase 2 (SOD2) were measured for evaluating redox balance. Besides, pyruvate dehydrogenase kinase (PDK) and pyruvate dehydrogenase (PDH) were detected to present the change in energetic metabolism during differentiation. To explore the effect of the mitochondrial metabolism on regulating hair regeneration, hair growth was observed after application of a mitochondrial respiratory inhibitor upon hair plucking. **Results.** During HFSCs differentiation, mitochondria became elongated with more abundant organized cristae and showed higher activity in differentiated cells. SOD2 was enhanced for redox balance with relatively poised ROS expression levels in differentiated cells. PDK increased in HFSCs while differentiated cells showed enhanced PDH, indicating that respiration converted from glycolysis to oxidative phosphorylation during differentiation. Inhibiting mitochondrial respiration in differentiated hair follicle cells upon hair plucking held back hair regeneration in vivo. **Conclusions.** Upon HFSCs differentiation, mitochondria was elongated with more abundant cristae and showed higher activity, accompanied with activated aerobic respiration in differentiated cells for higher energy supply. And dysfunction of mitochondrial respiration delays hair regeneration upon injury.

Mitochondrial aerobic respiration is activated during hair follicle stem cells differentiation and its dysfunction retards hair regeneration

Author name and affiliations

Yan Tang*, Binping Luo*, Zhili Deng, Ben Wang, Fangfen Liu, Jinmao Li, Wei Shi, Hongfu Xie, Ji Li.

Department of Dermatology, Xiangya Hospital, Central South University, Changsha, Hunan, China.

*Co-first author

Corresponding author:

Ji Li

87 Xiangya Road, Kaifu District, Changsha, Hunan, 410008, China.

Email address: Lydia.1208@hotmail.com

Abstract

Background. Emerging researches revealed the essential role of mitochondria in regulating stem/progenitor cell differentiation of neural progenitor cells, mesenchymal stem cells and other stem cells through reactive oxygen species (ROS), Notch or other signaling pathway. And inhibition of mitochondrial synthesis protein resulted in extension of hair loss upon injury. However, alteration of mitochondrial morphology and metabolic function during hair follicle stem cells (HFSCs) differentiation and how it affects hair regeneration has not been elaborated.

Methods. We compared the difference between telogen bulge cells and anagen matrix cells in mitochondrial morphology and activity. Expression levels of mitochondrial ROS and superoxide dismutase 2 (SOD2) were measured for evaluating redox balance. Besides, pyruvate dehydrogenase kinase (PDK) and pyruvate dehydrogenase (PDH) were detected to present the change in energetic metabolism during differentiation. To explore the effect of the mitochondrial metabolism on regulating hair regeneration, hair growth was observed after application of a mitochondrial respiratory inhibitor upon hair plucking.

Results. During HFSCs differentiation, mitochondria became elongated with more abundant organized cristae and showed higher activity in differentiated cells. SOD2 was enhanced for redox balance with relatively poised ROS expression levels in differentiated cells. PDK increased in HFSCs while differentiated cells showed enhanced PDH, indicating that respiration converted from glycolysis to oxidative phosphorylation during differentiation. Inhibiting mitochondrial respiration in differentiated hair follicle cells upon hair plucking held back hair regeneration in vivo.

Conclusions. Upon HFSCs differentiation, mitochondria was elongated with more abundant cristae and showed higher activity, accompanied with activated aerobic respiration in differentiated cells for higher energy supply. And dysfunction of mitochondrial respiration delays hair regeneration upon injury.

Introduction

Hair follicle (HF) is a cystic tissue surrounding the hair root controlling hair growth, consisting of two parts: an epithelial part (hair matrix and outer root sheath) and a dermal part (dermal papilla and connective tissue sheath). The hair follicle goes through cycles of anagen phase (growth), catagen phase (degeneration) and telogen phase (rest). (Stenn 2001) Hair follicle stem cells (HFSCs) have a slow cell cycle and play a crucial role in hair growth, regeneration of epidermis and sebaceous glands, and skin reparation after injury. (Varum et al. 2011). In late telogen, hair follicle bulge stem cells differentiate into matrix cells upon stimulation, entering the anagen phase. While in catagen phase, proliferation and differentiation of hair follicle cells gradually terminates, leaving with HFSCs and a dormant hair germ, recurring back to telogen phase. (Lien et al. 2011)

Stem cells such as hematopoietic stem cells (HSCs), embryonic stem cells (ESCs) and induced pluripotent stem cells (iPSCs) depend mostly on anaerobic metabolism rather than on aerobic metabolism, while terminally differentiated cells adopt aerobic respiration.(Hsu 2013; Jang et al. 2015; Kondoh et al. 2007; Teslaa 2015; Varum et al. 2011) As an essential organelle for anaerobic respiration, emerging research is focusing on the study of mitochondrial morphology and function during stem cell differentiation. First, mitochondria show less mass in ESCs than in differentiated cells and have a reduced oxygen consumption rate, accompanied with less ROS expression. (Cho et al. 2006; Choi et al. 2015; Lyu et al. 2008) Effective control of mitochondrial biological characteristics and function is critical for the maintenance of energy production and the prevention of damage by oxidative stress.(Parker et al. 2009) Besides,

mitochondria were found essential in deciding hair cell differentiation and proliferation upon injury through regulating energetic metabolism.(Armstrong et al. 2010; Hamanaka & Chandel 2013) During aerobic respiration, mitochondrial reactive oxygen species (ROS) are produced and inhibit stem cell differentiation and proliferation through redox signaling pathway.(Ghaffari 2008; Naka et al. 2008) For redox balance, expression of antioxidants such as SOD2 increases subsequently.

Interestingly, inhibition of mitochondrial protein synthesis increases area of hair loss by 30%-80%.(Gregory E. Hyde 1995) But the mechanism behind this phenomenon has not been fully illuminated. Recently, increasing studies have revealed the significance of mitochondria in regulating stem/progenitor cell differentiation and cell proliferation of keratinocytes, neural progenitor cells (NPCs) and bone marrow derived mesenchymal stem cells (bmMSCs). (Hamanaka & Chandel 2013; Kasahara & Scorrano 2014; Kloepper et al. 2015) However, the changes in mitochondrial morphology and function, especially bioenergetics metabolism during HFSC differentiation are rarely stated.

Hence, in this paper, we explored the alterations in mitochondrial morphology and activity during HFSCs differentiation and the effect of mitochondrial function in regulating hair regeneration. A more mature mitochondrial ultrastructure showing elongation with abundant organized cristae, and an increased mitochondrial activity were discovered in hair follicle cells upon differentiation. Antioxidant SOD2 was enhanced for maintaining the redox homeostasis during differentiation. Furthermore, inhibiting mitochondrial aerobic respiration held back hair regeneration after plucking.

85

86 # Materials and Methods

87 **Experimental animals**

88 C57BL/6 mice aged eight-week old were used in all experiments except the old mice group
89 (aged two-year old). All experiments were repeated at least three times with 3-5 mice each time.
90 All animals received humane care, maintaining in separated cages with general rodent diet under
91 the room temperature of 22 °C -24 °C.

92 The study was approved by the Ethics Committee of the Center, Scientific Research Center
93 with Animal Models, Xiangya Hospital, Central South University (No: 2011-01-05). All
94 procedures on animals followed the guidelines for humane treatment set by the Ethics
95 Committee of the Center, Scientific Research Center with Animal Models, Xiangya Hospital,
96 Central South University.

97

98 **Preparation of tissue samples**

99 Ketamine (80 mg/kg per mice) and Xylazine (5 mg/kg per mice) were injected i.p. before
100 tissue preparation. The skin samples with different phases of hairs were cut from the back of
101 mice after anesthesia, and the wound was sewed afterwards. Then the skin samples were
102 incubated in 0.25% solution of Dispase (Dispase I, Sigma-Aldrich Co. LLC) in Hanks' balanced
103 salt solution (HBSS, Life technologies, Thermo fisher Scientific Inc.,Grand Island, NY) at 4 °C
104 overnight. Due to previous research, hair follicles represent grey or black in anagen phase, while
105 showing pink with no pigment during telogen phase. (Maksim V. Plikus 2009) And the

epidermis with telogen hair follicles or anagen hair follicles was separated with forceps under a binocular light microscope according to skin color and underscopic morphology.

MitoTracker

The telogen hair follicles with epidermis and the whole anagen hair follicles were incubated in 50 nM MitoTracker media (MitoTracker® Red CMXRos, Life technologies, Thermo fisher Scientific Inc.) for 30 min at 37 ºC. After incubation and washing, the tissues were incubated with 3 uM DAPI (DAPI, 4', 6- Diamidino-2-Phenylindole, Dilactate, Life technologies, Thermo fisher Scientific Inc., Grand Island, NY) in PBS for 10 min at room temperature. Then the samples were put on the glass slide covered with glycerol and observed with a con-focal microscope.

Transmission electron microscope (TEM)

Immediately after removal of the mouse skin, tissues were sliced into small size samples (1 mm^3) and fixed in 3% buffered glutaraldehyde (Glutaraldehyde 25% solution, Sigma-Aldrich Co. LLC) for 4 h at 4 °C. Tissue specimens were then fixed in 1% osmium tetroxide (OsO^4, ReagentPlus®, 99.8%, Sigma-Aldrich Co. LLC) for 90 min. Fixed tissue was dehydrated using ascending grades of ethanol and then tissue was transferred into the resin via propylene oxide. After impregnation with pure resin, specimens were embedded in the same resin mixture. Ultra-thin sections of silver shades (60–70 nm) were cut using an ultra-microtome (Leica Rotary Microtome RM2255, Leica, UCT) equipped with a diamond knife; sections were then placed on copper grids and stained with uranyl acetate (20 min) and lead citrate (5 min). Stained sections were observed with a TEM (JEOL JEM-1011) operating at 80 kV.

Detection of ROS

The telogen hair follicles with epidermis and the whole anagen hair follicles were washed with PBS and treated with 10 μM DCFDA (29,79-dichlorofluorescein diacetate, DCFDA-Cellular Reactive Oxygen Species Detection Assay Kit, AbcamInc., Cambridge, MA.) in DMEM (Dulbecco's Modified Eagle Medium, Life technologies, Thermo fisher Scientific Inc.) for 20 min at 37 ºC in the dark. The samples were washed with PBS for 4 times and then put on a glass slide covered with glycerol and observed with a confocal microscopy.

Immunohistochemical Staining and Immunofluorescence staining

First, the skin samples were fixed in 4% Paraformaldehyde overnight at 4 ºC and then embedded with paraffin. After deparaffin and hydration, the samples sections were treated in boiling 0.01 M Tri-Sodium Citrate buffer (pH 6.0) for 20 min in water bath for antigen retrieval. And the samples were then incubated in 3% H_2O_2 at room temperature (22 ℃-24 ℃) for 10 min to quench endogenous peroxidase. Immunostaining procedure was carried out according to the manufacturer's instructions for the M.O.M kit (Cat No. PK-220; Vector Laboratories Inc., Burlingame, CA). The samples were incubated with primary antibodies for rabbit anti-SOD1 (1:200, Abcam Inc., Cambridge, MA) or mouse anti-SOD2 (1:200, Abcam Inc., Cambridge, MA) overnight at 4 ºC. The DAB substrate kit (Abcam Inc., Cambridge, MA) was used following for color development.

Early anagen hair follicles with epidermis were fixed in 100% methanol for 1 hr. Fixed samples were treated with 0.5% triton X-100 for 15 min at room temperature (22 ℃-24 ℃) and then blocked with 5% bovine serum albumin for 1 hr at 37 °C. After rinsing with PBS, the

148 samples were incubated at 4 °C overnight with PDK or PDH antibodies (1:200, Santa cruz
149 biotechnology Inc.), and then K15 or Ki67 primary antibodies respectively at 37 °C for 1 hr.
150 Samples were rinsed with PBS for 4 times (5 min each time) and then incubated in the dark for 1
151 hr at 37 °C with two appropriate fluorescence-labeled secondary antibodies respective to the
152 primary antibodies. After rinsing with PBS for 4 times (5 min each time), the samples were
153 incubated with 3 μM DAPI in PBS and then were put on glass slides covered with glycerol and
154 observed with con-focal microscopy.

155 Length of mitochondria was measured through Image pro plus 6.0. Integrated optical
156 density (IOD) and area of figures were evaluated by Image pro plus 6.0, and mean density was
157 calculated as following standard method (Mean density = IOD/area). A two-tailed student's t test
158 was used for comparison.

159 **Drug preparation**

160 Antimycin A (Sigma-Aldrich Co. LLC) was prepared at 1 M as a stock solution in DMSO,
161 and then diluted with DMEM to a final concentration of 10 μM prior to use.

162 **Hair regeneration in vivo**

163 Synchronous anagen was induced by depilation in the back skin of mice with all dorsal skin
164 HFs in telogen stage of the hair cycle as described by Muller-Rover et al.(Porter 2003) After HFs
165 switched from anagen to telogen, we injected 100 μl antimycin A (experiment group; prepared
166 with DMSO) and DMSO (control group) intracutaneously on respective side of the mouse back
167 for 10 days and plucked 200 hairs at the drug treated sites at the 3rd day of treatment (Day 3). In
168 this experiment, mice were separated in different cages (1 mice per cage) and they were under

close observation everyday. Pictures were taken of the studied location on mouse back every day and recorded the time when the hair grows out.

Statistical analysis

Non-parametric Mann Whitney test was performed for comparison through GraphPad Prism 6.0 software. A value of $P < 0.05$ was considered statistically significant.

Results

Change of mitochondrial ultrastructure during hair follicle bulge cells differentiation

During telogen phase, the inferior part of the hair follicle consists of mostly bulge stem cells and secondary hair germ. (Mayumi Ito 2004) Then, the bulge stem cells differentiate into proliferating matrix cells, entering the anagen phase. (Caroline Wilson 1994; Hideo Oshima 2001) Hence in this paper, telogen phase hair follicle bulge cells (abbreviated as telogen bulge cells) and anagen phase proliferating hair follicle matrix cells (abbreviated as anagen matrix cells) were used as representative of HFSCs and differentiated HF cells respectively to detect the change in mitochondrial morphology and function during HFSCs differentiation.

First, mitochondrial morphology was observed with electron microscopy. In ultrastructure, mitochondria were discrete and spherical in telogen bulge cells (Fig. 1b) with less cristae (Fig. 1d), while in anagen matrix cells more in number and elongated (Fig. 1a) with organized cristae (Fig. 1c). And the average length of mitochondria in anagen matrix cells was significantly increased than that in telogen bulge cells (Fig. 1e). Accordingly, the mitochondria became more

189 mature in ultrastructure after differentiation, implying that differentiated matrix cells have a
190 higher energetic potential.
191
192 **Fig. 1. Mitochondria are elongated with abundant cristae in anagen matrix cells.**
193 Magnifications of (a) 10x, and (c) 20x of mitochondria ultrastructure in anagen phase
194 differentiated hair follicle matrix cells. More elongated mitochondria shown in (a) anagen phase,
195 while more discrete, spherical mitochondria shown in (b) telogen phase bulge cells. (Marked by
196 red arrows) Magnifications of (b) 10x, and (d) 20x of mitochondria ultrastructure in telogen
197 phase bulge cells. Mitochondria in (c) anagen phase matrix cells showed more abundant cristae
198 than in (d) telogen phase bulge cells. (Marked by red arrows) (e) The lengths of Mitochondria
199 measured in anagen matrix cells were significantly shorter than in telogen bulge cells. (**, $P <$
200 0.01) Data show a complication of 3 experiments (n=4 mice per group, with two 5mm x 5mm
201 sections per mice).
202
203 **Alteration of mitochondrial activity in HFSCs differentiation**
204 It was previously observed that iPSCs typically have glycolytic energy production at
205 pluripotent phase, whereas mitochondrial oxidative phosphorylation is essential during cell
206 proliferation and differentiation. Besides reduced energy metabolism, iPSCs also have less
207 mitochondria and lower mitochondrial activity than those in differentiated cells. The alteration of
208 the mitochondrial morphology and function are crucial markers of iPSCs differentiation. (Varum
209 et al. 2011) However, the change of mitochondrial activity during HFSCs differentiation has not

been elucidated.

Thus mitochondrial activity was assessed using Mito Tracker Red. Due to our result, fluorescence intensity was significantly increased in anagen matrix cells compared with telogen bulge cells (Fig. 2a). Keratin 15 (K15) is known as a marker for stem cells while Ki67 symbolizes proliferating matrix cells. (Eisinger et al. 2010) To locate HFSCs and proliferating HF matrix cells precisely, K15 and Ki67 were detected as shown in Fig. 2b. And there is an approximately three times increase in the fluorescence intensity of Mitotracker Red in $Ki67^+$ proliferating cells than in $K15^+$ stem cells (Fig. 2b), suggesting an enhancement in mitochondrial activity during HFSCs differentiation, which is in accordance with the feature of embryonic stem cells. (Chung et al. 2007) In addition, mitochondrial activity in mice of the young group (8 week-old) does not differ from that of the old group (2 year-old) (Fig. 2c), indicating that ageing does not have an significant influence on mitochondrial activity during stem cell differentiation.

Fig. 2. Mitochondrial activity is increased in anagen proliferating matrix cells.

Fluorescence intensity of Mitotracker Red was detected to measure mitochondrial activity. (a) More mitochondria and a higher mitochondrial activity were detected in anagen matrix cells than in telogen bulge cells. (b) Mitochondrial activity was significantly elevated in $Ki67^+$ proliferating cells than in $K15^+$ stem cells (**, $P < 0.01$). (Markers flagged by white arrows) (c) Mitochondria in matrix cells were of same activity levels due to in different aged mice. (a, b) Data show a complication of 3 experiments (n=3 mice per group, with two 5 mm x 5 mm sections per mouse).

(c) Data show a complication of 3 experiments (n=three 8 week-old mice (young group) and three 2 year-old mice (old group) per experiment, with two 5 mm x 5 mm sections per mouse).

Redox balance was sustained through enhancing SOD2 expression

As mitochondrion is the major generator of endogenous ROS in cells, electrons that leak out from the electron transport chain contribute to the production of ROS. (Chien-Tsun Chen 2008) Here H2DCFDA (2', 7'-dichlorodihydrofluorescein diacetate) immunofluorescence was used to measure ROS levels in HFSCs. Unexpectedly, ROS expression is almost identical between these two stages of cell types (Fig. 3a). Nonetheless, expression of superoxide dismutase 2 (SOD2), an essential antioxidant enzyme, was significantly improved in anagen matrix cells compared with that in the telogen bulge cells (Fig. 3b). We speculate that SOD2 levels are upregulated in anagen matrix cells to clear ROS during the differentiation process for redox homeostasis. Expression of SOD1, another antioxidant enzyme, was also detected during HFSC differentiation, but showed no significant difference (data not shown).

Fig. 3. SOD2 is increased in anagen matrix cells to maintain redox homeostasis.

(a). There was no significant difference in ROS expression between telogen bulge cells and anagen matrix cells (P >0.05). (b). SOD2 expression was significantly enhanced in anagen matrix cells. (*, P <0.05). Data show a complication of 3 experiments (n=3 mice per group, with two 5 mm x 5 mm sections per mouse).

Variation of respiratory enzymes expression during HFSCs differentiation

To further check the type of metabolism used by HFSCs, we again detected respiratory enzymes in $K15^+$ stem cells and that of $Ki67^+$ proliferating cells. As shown in Fig. 4, PDK was highly expressed in HFSCs (Fig. 4a) while PDH was highly expressed in differentiated cells (Fig. 4b), indicating that anaerobic mitochondrial metabolism plays a dominant role in HFSCs, whereas aerobic metabolism is essential in differentiated cells.

Fig. 4. HFSCs present anaerobic respiration, while proliferating matrix cells show oxidative phosphorylation.

Immunofluorescence detection of PDK and PDH during HFSC differentiation. (a). PDK is mainly expressed in $K15^+$ stem cells. (b). PDH is mainly expressed in $Ki67^+$ proliferating cells. Data show a complication of 3 experiments (n=5 mice per group, with two 5 mm x 5 mm sections per mouse).

Suppressing mitochondrial oxidative phosphorylation delays hair regeneration

Oxidative phosphorylation increases during HFSCs differentiation, which is supplied mainly via the mitochondrial respiratory pathway (Armstrong et al. 2010). It is temping to speculate that disrupting mitochondrial oxidative phosphorylation might inhibit the differentiation and proliferation of hair stem cells and retard hair regeneration. Hence, a mitochondrial respiratory inhibitor, antimycin A [complex III inhibitor], was injected on one side of mouse dorsal skin subcutaneously to prohibit mitochondrial activity. And DMSO was treated

on the contralateral side as the control group. The treatment process is summarized in Fig. 5a. 200 hairs were plucked after three days of drug treatment. After plucking, hair regrowth was recorded in these treated regions and the appearance of neonatal hair by taking photographs each day (Fig. 5b). The antimycin A group showed significant delays (9.6 ± 0.9 days) in hair growth compared with the DMSO group (6.7 ± 0.7 days), as shown in Fig. 5c (P <0.05). Accordingly, disruption of mitochondrial respiration leads to delay of hair follicle regrowth, revealing that alteration of mitochondrial respiratory function might be essential in HFSCs differentiation.

Fig. 5. Inhibiting mitochondrial respiration retards hair regrowth.

(a). Schematic diagram of our experimental approach. Mice were treated with Antimycin A intracutaneously on one side of the back skin, and DMSO on the contralateral side for 10 days. 200 hairs were plucked after three days of drug treatment (as shown in red arrow). Photos were taken at day 3, day 11 and day 19 after the start of treatment (as shown in blue arrow). (b). Photos of hair regrowth taken at day 3, 11, and 19 after treatment. At day 11, hair growth was observed in the DMSO treatment group (control group) while hairs failed to grow in the antimycin A treatment group, indicating that hair regeneration was held back in the antimycin A group. (c). It took much longer time in the antimycin A group (9.6 ± 0.9 days) in hair regrowth than that in the DMSO group (6.7±0.7 days) (**, P < 0.01). Data show a complication of 3 experiments (n=3 mice per group).

Discussion

Emerging studies focus on the effect of mitochondria in regulating stem/progenitor cell differentiation and proliferation. For instance, mitochondrial ROS signal transduction was found of importance in regulating keratinocyte differentiation. (Hamanaka & Chandel 2013; Hamanaka et al. 2013) Plus, mitochondria negatively regulate proliferation and differentiation of embryonic mouse cerebral cortical neural progenitor cells (NPCs) through generating superoxide.(Yan Hou 2012) And differentiation of bmMSCs was accompanied by distinct regulation of mitochondrial bioenergetics, providing a novel way in manipulating cell fate of MSCs.(Shum et al. 2016) Crucially, deletion of mitochondrial transcription factor A (Tfam(EKO)), which induces loss of the electron transport chain (ETC) in epidermis, restrains entire skin development, including hair follicle differentiation and proliferation.(Kloepper JE 2015) Despite the importance of mitochondria in regulating cell differentiation, the alterations of mitochondrial morphology and its respiratory function during HFSCs differentiation are poorly stated. Hence, in this paper, we firstly explored the change in mitochondrial morphology and activity, redox homeostasis and metabolic bioenergetics of HFSCs during differentiation.

Mitochondria display cycles of fission and fusion, showing a dynamic morphology together with function.(Willems et al. 2015) Differentiated hair follicle cells demonstrated more mature mitochondrial ultrastructure with elongated shape ($P<0.01$) and more cristae protruding into the matrix than HFSCs. (Fig. 1) Simultaneously, differentiated hair follicle cells showed higher mitochondrial activity based on the fluorescence intensity of Mitotracker Red ($P<0.05$). (Fig. 2a) Furthermore, K15 and Ki67, biomarkers for epidermal stem cells and proliferating cells

313 respectively (Bose et al. 2013; Ohta Y 2000; Scholzen T 2000) were used for accurate location
314 of HFSCs and its differentiated counterparts. Again the result confirms the phenomenon as
315 described above that differentiated hair follicle cells have higher mitochondrial activity. (Fig. 2b)
316 It is previously revealed that mitochondria became elongated with swollen cristae in
317 differentiated ESCs to prepare for aerobic metabolism.(J. M. Facucho-Oliveira 2009)
318 Additionally, mitochondria increased and became more mature in ultrastructure as described
319 above in differentiation of human MSCs and human ESCs.(Chien-Tsun Chen 2008; Cho et al.
320 2006) Even in female primordial germ cell, mitochondria transform from rounded with small
321 vesicular cristae into elongated one with parallel, arched cristae upon differentiation.(Pietro
322 M.Motta 2000) Hence, it is supposed that mitochondrial ultrastructure and activity altered to
323 adapt to the demand of energy supply during HFSCs differentiation.

324 ROS, a principle production of mitochondrial metabolism, regulates the redox balance
325 along with antioxidants, such as SOD2. Also, ROS was discovered as a secondary signal
326 pathway in regulating cell differentiation, such as keratinocytes and neural progenitor cells. It is
327 reported promoting cell senescence such as bmMSCs as well. (Hamanaka et al. 2013; Junfang
328 Wu 2014; Yan Hou 2012) However, ROS expression was not significantly altered upon HFSCs
329 differentiation, showing no difference between telogen bulge stem cells and anagen
330 differentiated cells (Fig. 3a), though mitochondrial activity was distinctly increased. To better
331 present redox status, antioxidants SOD1 and SOD2 were also measured. Expression of SOD2
332 was upregulated during HFSCs differentiation (Fig. 3b), but SOD1 did not differ in the process
333 (data not shown). Elevated SOD2 expression during differentiation of iPSCs and neuroblastoma

cells was discovered in previous studies for sustaining redox homeostasis and preventing ROS-induced cell death, either. (Armstrong et al. 2010; Case AJ 2013; Ruggeri P 2014) Interestingly, enhanced mitochondrial activity upon HFSCs differentiation is age independent (Fig. 2c), while deletion of SOD2 results in diverse effect of mitochondrial dysfunction on epidermal stem cells between young and old mouse model.(Michael C. Velarde 2015) In addition, overexpression of SOD2 was proved to be protective in myoblast mitochondrial mass and function with ageing (Lee S 2009), indicating that mitochondrial activity and function might be preserved by SOD2 expression when ageing due to our result. All above prompted us the essential role of SOD2 in maintaining the redox homeostasis.

Except for redox homeostasis, mitochondrial metabolic function is of great importance in regulating hair growth. As is known, PDH is responsible for the conversion of pyruvate into acetyl CoA to enter the tricarboxylic acid cycle and aerobic metabolism, while PDK inhibits its activity by phosphorylation, representing aerobic and anaerobic respiration respectively. Hence PDH and PDK were measured in HFSCs and differentiated HF cells for measurement of respiration. HFSCs conducted anaerobic glycolysis, while switched into oxidative phosphorylation in differentiated cells in our results, revealing an anaerobic-aerobic transition pattern (Fig. 4). Similarly, oxidative phosphorylation was activated in MSCs during osteogenic differentiation.(Shum et al. 2016) To explore the significance of alteration in mitochondrial energetic metabolism during differentiation, antimycin A (a mitochondrial respiratory inhibitor) was used in vivo followed by hair pluck at the third day. The results revealed that disrupting mitochondrial respiration delays hair regrowth after plucking (Fig. 5). The mechanism needs

355 further exploration. A possibility is that hair regeneration might be retarded due to insufficient
356 energy supply. Another possibility is that mitochondrial dysfunction affects HFSCs
357 differentiation through regulating redox balance or other signaling pathways, leading to delay of
358 hair growth. Mitochondria make pleiotropic effects on cell differentiation through different
359 signaling pathways. For instance, down-regulation of DRP suppresses Notch and subsequently
360 suppressing follicle cell differentiation in *Drosophilia*. mROS inhibits epidermal differentiation
361 through decreasing Notch signaling. Furthermore, inhibiting nuclear translocation of apoptosis-
362 inducing factor (AIF), which was released from mitochondria, retards anagen-to-catagen phase
363 transition of hair follicle growth cycle and leads to decrease in hair regeneration. (Lan S 2015)
364 Therefore, further research is needed to reveal if mitochondrial metabolic dysfunction inhibits
365 hair regeneration through regulating HFSCs cell differentiation and its signaling pathway.
366

367 # Conclusion

368 In summary, mitochondria are elongated with parallel, arched cristae and show higher
369 activity in differentiated hair follicle cells. SOD2 increases to maintain redox homeostasis,
370 preventing from ROS induced injury. Plus, HFSCs present anaerobic glycolysis at juvenile phase,
371 while show mitochondrial oxidative phosphorylates after differentiation. And inhibiting
372 mitochondrial metabolic function retards hair regeneration.
373

374 # Additional Information and Declarations

375 **Acknowledgments**

376 Thank Dr. Cheng-Ming Chuong for his support in our experiments.

References

Armstrong L, Tilgner K, Saretzki G, Atkinson SP, Stojkovic M, Moreno R, Przyborski S, and Lako M. 2010. Human induced pluripotent stem cell lines show stress defense mechanisms and mitochondrial regulation similar to those of human embryonic stem cells. *Stem Cells* 28:661-673. 10.1002/stem.307

Bose A, Teh MT, Mackenzie IC, and Waseem A. 2013. Keratin k15 as a biomarker of epidermal stem cells. *Int J Mol Sci* 14:19385-19398. 10.3390/ijms141019385

Caroline Wilson GC, Zhi-Gang Wei, Eric Fryer, Jennifer Margolis-Fryer, Matt Ostead, Robert Tokarek, Tung-Tien Sun andRobert M. Lavker. 1994. Cells within the bulge region of mouse hair follicle transiently proliferate during early anagen: heterogeneity and functional differences of various hair cycles. *Differentiation* 55:127-136.

Case AJ MJ, Motto DG, Meyerholz DK, Domann FE. 2013. Manganese superoxide dismutase depletion in murine hematopoietic stem cells perturbs iron homeostasis, globin switching, and epigenetic control in erythrocyte precursor cells. *Free Radic Biol Med* 56:17-27.

Chien-Tsun Chen Y-RVS, Tom K. Kuo, Oscar K. Lee, Yau-Huei Wei. 2008. Coordinated chages of mitochondrial biogenesis and antioxidant enzymes during osteogenic differentiation of human mesenchymal stem cells. *Stem Cells* 26:960-968. 10.1634/stemcells.2007-

Cho YM, Kwon S, Pak YK, Seol HW, Choi YM, Park do J, Park KS, and Lee HK. 2006. Dynamic changes in mitochondrial biogenesis and antioxidant enzymes during the spontaneous differentiation of human embryonic stem cells. *Biochem Biophys Res Commun* 348:1472-1478. 10.1016/j.bbrc.2006.08.020

Choi HW, Kim JH, Chung MK, Hong YJ, Jang HS, Seo BJ, Jung TH, Kim JS, Chung HM, Byun SJ, Han SG, Seo HG, and Do JT. 2015. Mitochondrial and metabolic remodeling during reprogramming and differentiation of the reprogrammed cells. *Stem Cells Dev*. 10.1089/scd.2014.0561

Chung S, Dzeja PP, Faustino RS, Perez-Terzic C, Behfar A, and Terzic A. 2007. Mitochondrial oxidative metabolism is required for the cardiac differentiation of stem cells. *Nat Clin Pract Cardiovasc Med* 4 Suppl 1:S60-67. 10.1038/ncpcardio0766

Eisinger M, Li WH, Rossetti DD, Anthonavage M, and Seiberg M. 2010. Sebaceous gland regeneration in human skin xenografts. *J Invest Dermatol* 130:2131-2133. 10.1038/jid.2010.122

Ghaffari S. 2008. Oxidative stress in the regulation of normal and neoplastic hematopoiesis. *Antioxid Redox Signal* 10:1923-1940. 10.1089/ars.2008.2142

Gregory E. Hyde aEWR. 1995. Mitochondrial role in hair cell survival after injury. *Otolaryngol Head Neck Surg* 113:530-540.

Hamanaka RB, and Chandel NS. 2013. Mitochondrial metabolism as a regulator of keratinocyte differentiation. *Cell Logist* 3:e25456. 10.4161/cl.25456

Hamanaka RB, Glasauer A, Hoover P, Yang S, Blatt H, Mullen AR, Getsios S, Gottardi CJ, DeBerardinis RJ, Lavker RM, and Chandel NS. 2013. Mitochondrial reactive oxygen species promote epidermal differentiation and hair follicle development. *Sci Signal* 6:ra8. 10.1126/scisignal.2003638

Hideo Oshima AR, Ce cile Kedzia, Koji Kobayashi, and Yann Barrandon. 2001. Morphogenesis and Renewal of Hair Follicles from Adult Multipotent Stem Cells. *Cell* 104:233-245.

Hsu PQ, Cheng-Kui. 2013. Metabolic plasticity and hematopoietic stem cell biology. *Curr Opin Hematol* 20:289-294. 10.1097/MOH.0b013e328360ab4d

418 J. M. Facucho-Oliveira JCSJ. 2009. The Relationship Between Pluripotency and Mitochondrial DNA Proliferation
419 During Early Embryo Development and Embryonic Stem Cell Differentiation. *Stem Cee Rev and Rep*
420 5:140-158.
421 Jang H, Yang J, Lee E, and Cheong JH. 2015. Metabolism in embryonic and cancer stemness. *Arch Pharm Res*.
422 10.1007/s12272-015-0558-y
423 Junfang Wu JN, Xiaopeng Li, Xianwei Wang, Zhikun Guo and Fenxi Zhang. 2014. TGF-β 1 induces senescence of
424 bone marrow mesenchymal stem cells via increase of mitochondrial ROS production. *BMC Dev Biol* 14.
425 Kasahara A, and Scorrano L. 2014. Mitochondria: from cell death executioners to regulators of cell differentiation.
426 *Trends Cell Biol* 24:761-770. 10.1016/j.tcb.2014.08.005
427 Kloepper JE, Baris OR, Reuter K, Kobayashi K, Weiland D, Vidali S, Tobin DJ, Niemann C, Wiesner RJ, and Paus
428 R. 2015. Mitochondrial function in murine skin epithelium is crucial for hair follicle morphogenesis and
429 epithelial-mesenchymal interactions. *J Invest Dermatol* 135:679-689. 10.1038/jid.2014.475
430 Kloepper JE BO, Reuter K, Kobayashi K, Weiland D, Vidali S, Tobin DJ, Niemann C, Wiesner RJ, Paus R. 2015.
431 Mitochondrial function in murine skin epithelium is crucial for hair follicle morphogenesis and epithelial-
432 mesenchymal interactions. *J Invest Dermatol* 135:679-689.
433 Kondoh H, Lleonart ME, Nakashima Y, Yokode M, Tanaka M, Bernard D, Gil J, and Beach D. 2007. A High
434 Glycolytic Flux Supports the Proliferative Potential of Murine Embryonic Stem Cells. *Antioxidants &*
435 *Redox Signaling* 9:293-299. 10.1089/ars.2006.1467
436 Lan S LF, Zhao G, Zhou T, Wu C, Kou J, Fan R, Qi X, Li Y, Jiang Y, Bai T, Li P, Liu L, Hao D, Zhang L, Li Y,
437 Liu JY. 2015. Cyclosporine A increases hair follicle growth by suppressing apoptosis-inducing factor
438 nuclear translocation: a new mechanism. *Fundam Clin Pharmacol* 29:191-203.
439 Lee S VRH, Csete M. 2009. Sod2 overexpression preserves myoblast mitochondrial mass and function, but not
440 muscle mass with aging. *Aging Cell* 8:196-310.
441 Lien WH, Guo X, Polak L, Lawton LN, Young RA, Zheng D, and Fuchs E. 2011. Genome-wide maps of histone
442 modifications unwind in vivo chromatin states of the hair follicle lineage. *Cell Stem Cell* 9:219-232.
443 10.1016/j.stem.2011.07.015
444 Lyu BN, Ismailov SB, Ismailov B, and Lyu MB. 2008. Mitochondrial concept of leukemogenesis: key role of
445 oxygen-peroxide effects. *Theor Biol Med Model* 5:23. 10.1186/1742-4682-5-23
446 Maksim V. Plikus aC-MC. 2009. Complex hair cycle domain patterns and regenerative hair waves in living rodents.
447 *J Invest Dermatol* 128:1071-1080.
448 Mayumi Ito GC, Kenji Kizawa, Kazuto Hamada. 2004. Hair follicle stem cells in the lower bulge form the
449 secondary germ, a biochemically distinct but functionally equivalent progenitor cell population, at the
450 termination of catagen. *Differentiation* 72:548-557.
451 Michael C. Velarde MD, Simon Melov, and Judith Campisi. 2015. Pleiotropic age-dependent effects of
452 mitochondrial dysfunction on epidermal stem cells. *Proc Natl Acad Sci USA* 112:10407-10412.
453 Naka K, Muraguchi T, Hoshii T, and Hirao A. 2008. Regulation of reactive oxygen species and genomic stability in
454 hematopoietic stem cells. *Antioxid Redox Signal* 10:1883-1894. 10.1089/ars.2008.2114
455 Ohta Y IK. 2000. Proliferation markers, proliferating cell nuclear antigen, Ki67, 5-bromo-2'-deoxyuridine, and
456 cyclin D1 in mouse olfactory epithelium. *Ann Otol Rhinol Laryngol* 109:1046-1048.
457 Parker GC, Acsadi G, and Brenner CA. 2009. Mitochondria: determinants of stem cell fate? *Stem Cells Dev* 18:803-
458 806. 10.1089/scd.2009.1806.edi

Pietro M.Motta SAN, Sayoko Makabe, Rosemarie Heyn. 2000. Mitochondrial morphology in human fetal and adult female germ cells. *Human Reproduction* 15:129-147.

Porter RM. 2003. Mouse models for human hair loss disorders. *J Anat* 202:125-131.

Ruggeri P FA, Di Ianni N, Cappabianca L, Ragone M, Ianni G, Gulino A, Mackay AR. 2014. The TrkAIII oncoprotein inhibits mitochondrial free radical ROS-induced death of SH-SY5Y neuroblastoma cells by augmenting SOD2 expression and activity at the mitochondria, within the context of a tumour stem cell-like phenotype. *PLoS One* 9.

Scholzen T GJ. 2000. The Ki-67 protein: from the known and the unknown. *J Cell Physiol* 182:311-322.

Shum LC, White NS, Mills BN, de Mesy Bentley KL, and Eliseev RA. 2016. Energy Metabolism in Mesenchymal Stem Cells During Osteogenic Differentiation. *Stem Cells Dev* 25:114-122. 10.1089/scd.2015.0193

Stenn KS, and R. Paus. 2001. Controls of Hair Follicule Cycling. *Physiological Reviews* 81:449-494.

Teslaa T, Teitell, Michael A. 2015. Pluripotent stem cell energy metabolism: an update. *EMBO J* 34:138-153. 10.15252/embj.201490446

Varum S, Rodrigues AS, Moura MB, Momcilovic O, Easley CAt, Ramalho-Santos J, Van Houten B, and Schatten G. 2011. Energy metabolism in human pluripotent stem cells and their differentiated counterparts. *PLoS One* 6:e20914. 10.1371/journal.pone.0020914

Willems PH, Rossignol R, Dieteren CE, Murphy MP, and Koopman WJ. 2015. Redox Homeostasis and Mitochondrial Dynamics. *Cell Metab* 22:207-218. 10.1016/j.cmet.2015.06.006

Yan Hou XO, Ruiqian Wan, Heping Cheng, Mark P. Mattson, and Aiwu Cheng. 2012. Mitochondrial Superoxide Production Negatively Regulates Neural Progenitor Proliferation and Cerebral Cortical Development. *Stem Cells* 30:2535-2547.

1

Mitochondria are elongated with abundant cristae in anagen matrix cells.

Fig. 1. Mitochondria are elongated with abundant cristae in anagen matrix cells. Magnifications of (a) 10x, and (c) 20x of mitochondria ultrastructure in anagen phase differentiated hair follicle matrix cells. More elongated mitochondria shown in (a) anagen phase, while more discrete, spherical mitochondria shown in (b) telogen phase bulge cells. (Marked by red arrows) Magnifications of (b) 10x, and (d) 20x of mitochondria ultrastructure in telogen phase bulge cells. Mitochondria in (c) anagen phase matrix cells showed more abundant cristae than in (d) telogen phase bulge cells. (Marked by red arrows) (e) The lengths of Mitochondria measured in anagen matrix cells were significantly shorter than in telogen bulge cells. (**, $P < 0.01$) Data show a complication of 3 experiments (n=4 mice per group, with two 5mm x 5mm sections per mice).

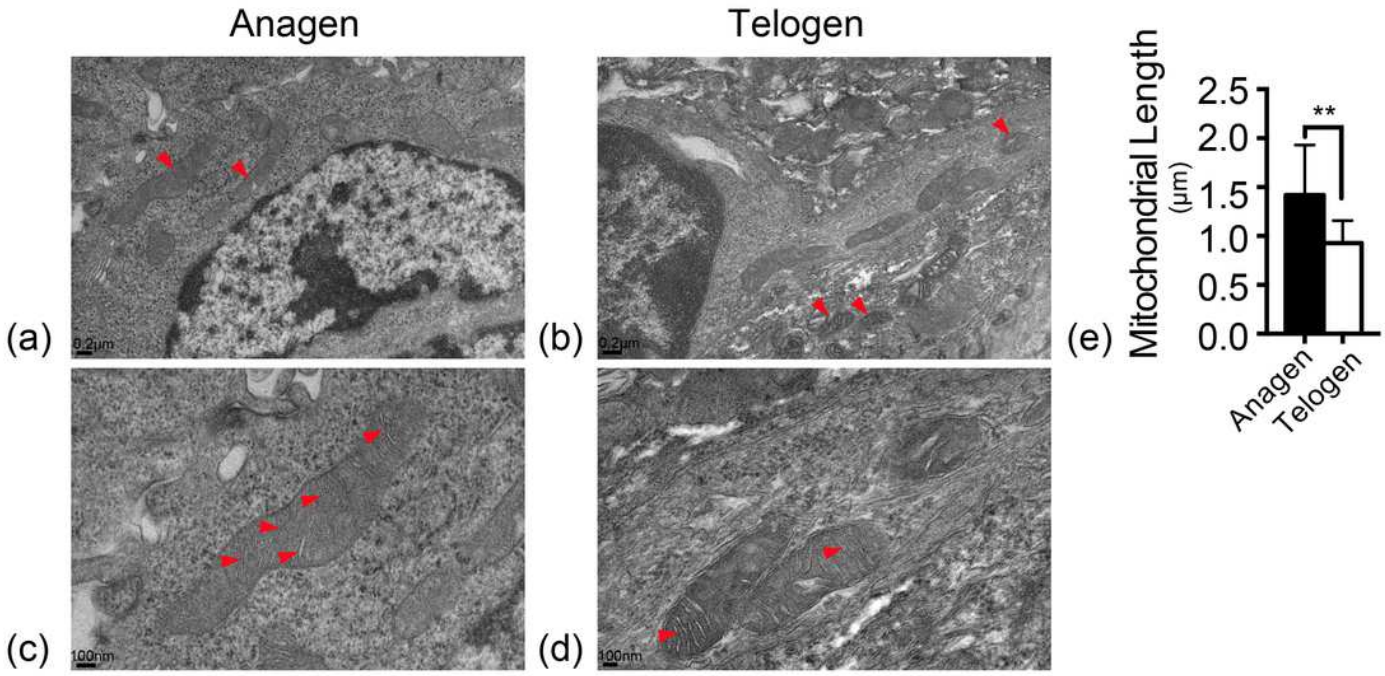

Mitochondrial activity is increased in anagen proliferating matrix cells.

Fig. 2. Mitochondrial activity is increased in anagen proliferating matrix cells. Fluorescence intensity of Mitotracker Red was detected to measure mitochondrial activity. (a) More mitochondria and a higher mitochondrial activity were detected in anagen matrix cells than in telogen bulge cells. (b) Mitochondrial activity was significantly elevated in $Ki67^{+}$ proliferating cells than in $K15^{+}$ stem cells (**, $P < 0.01$). (Markers flagged by white arrows) (c) Mitochondria in matrix cells were of same activity levels due to in different aged mice. (a, b) Data show a complication of 3 experiments (n=3 mice per group, with two 5 mm x 5 mm sections per mouse). (c) Data show a complication of 3 experiments (n=three 8 week-old mice (young group) and three 2 year-old mice (old group) per experiment, with two 5 mm x 5 mm sections per mouse).

PeerJ PrePrints | https://doi.org/10.7287/peerj.preprints.1769v1 | CC-BY 4.0 Open Access | rec: 22 Feb 2016, publ: 22 Feb 2016

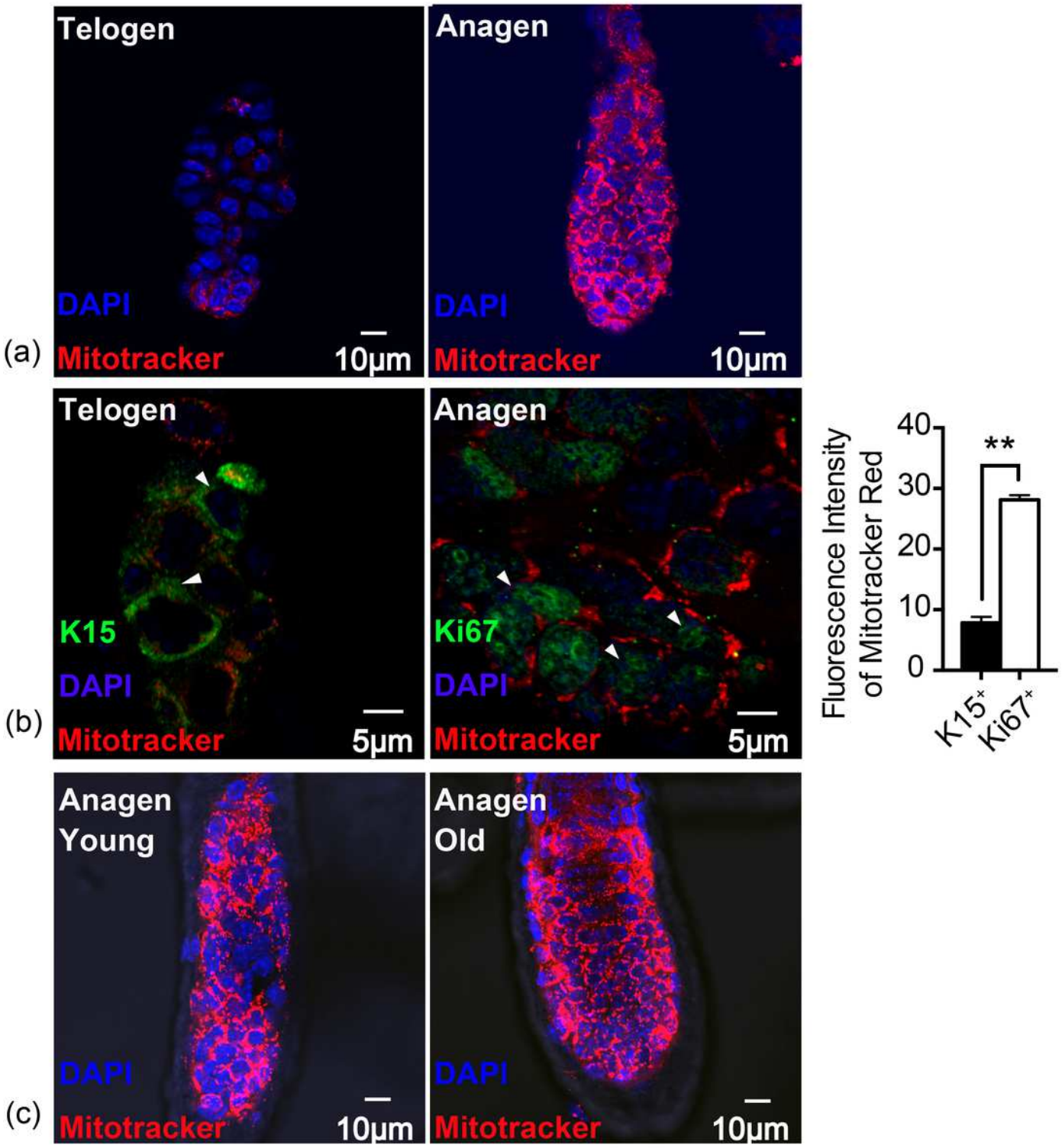

3

SOD2 is increased in anagen matrix cells to maintain redox homeostasis.

Fig. 3. SOD2 is increased in anagen matrix cells to maintain redox homeostasis. (a). There was no significant difference in ROS expression between telogen bulge cells and anagen matrix cells (P >0.05). (b). SOD2 expression was significantly enhanced in anagen matrix cells. (*, P <0.05). Data show a complication of 3 experiments (n=3 mice per group, with two 5 mm x 5 mm sections per mouse).

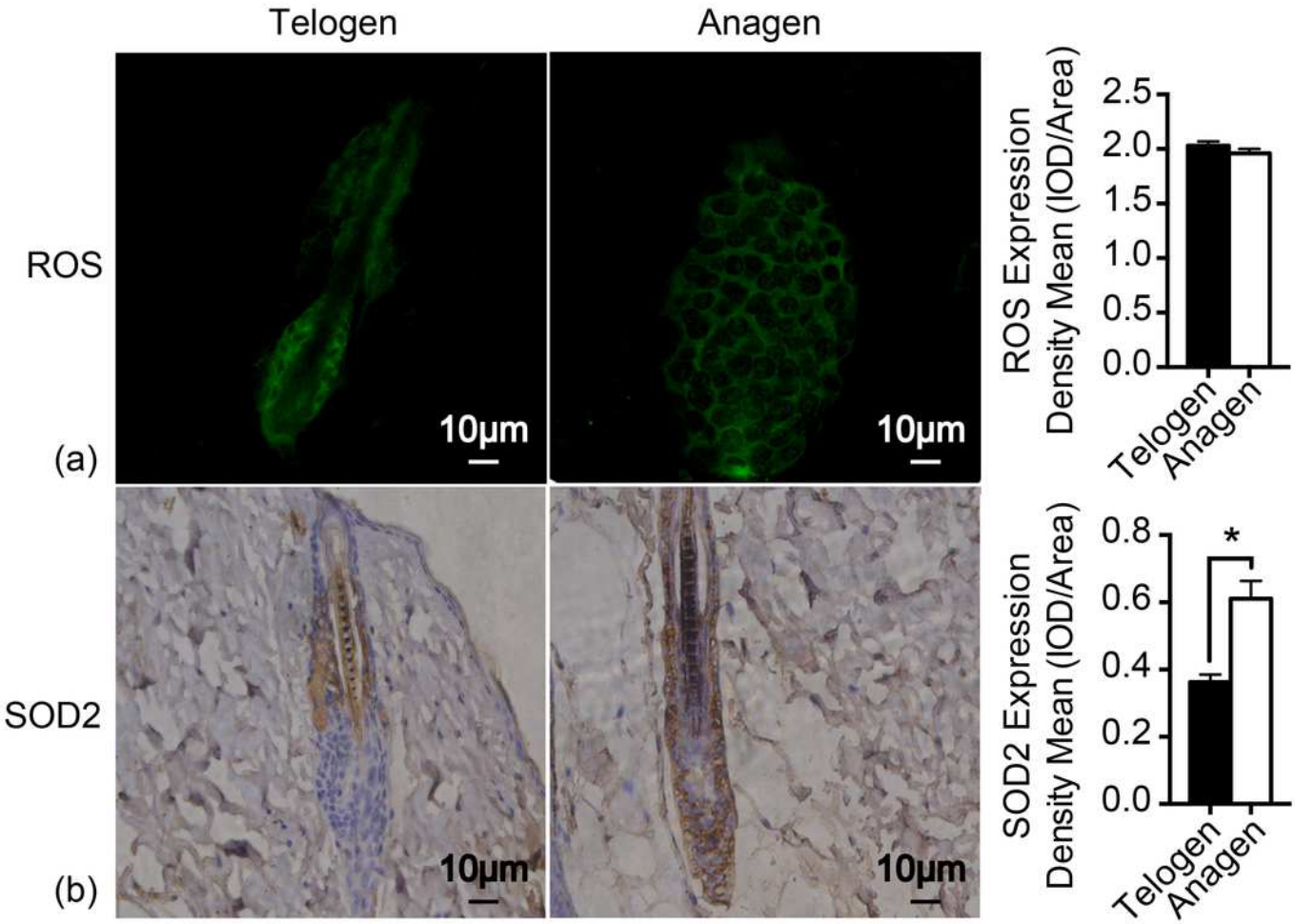

4

HFSCs present anaerobic respiration, while proliferating matrix cells show oxidative phosphorylation.

Fig. 4. HFSCs present anaerobic respiration, while proliferating matrix cells show oxidative phosphorylation. Immunofluorescence detection of PDK and PDH during HFSC differentiation. (a). PDK is mainly expressed in $K15^+$ stem cells. (b). PDH is mainly expressed in $Ki67^+$ proliferating cells. Data show a complication of 3 experiments (n=5 mice per group, with two 5 mm x 5 mm sections per mouse).

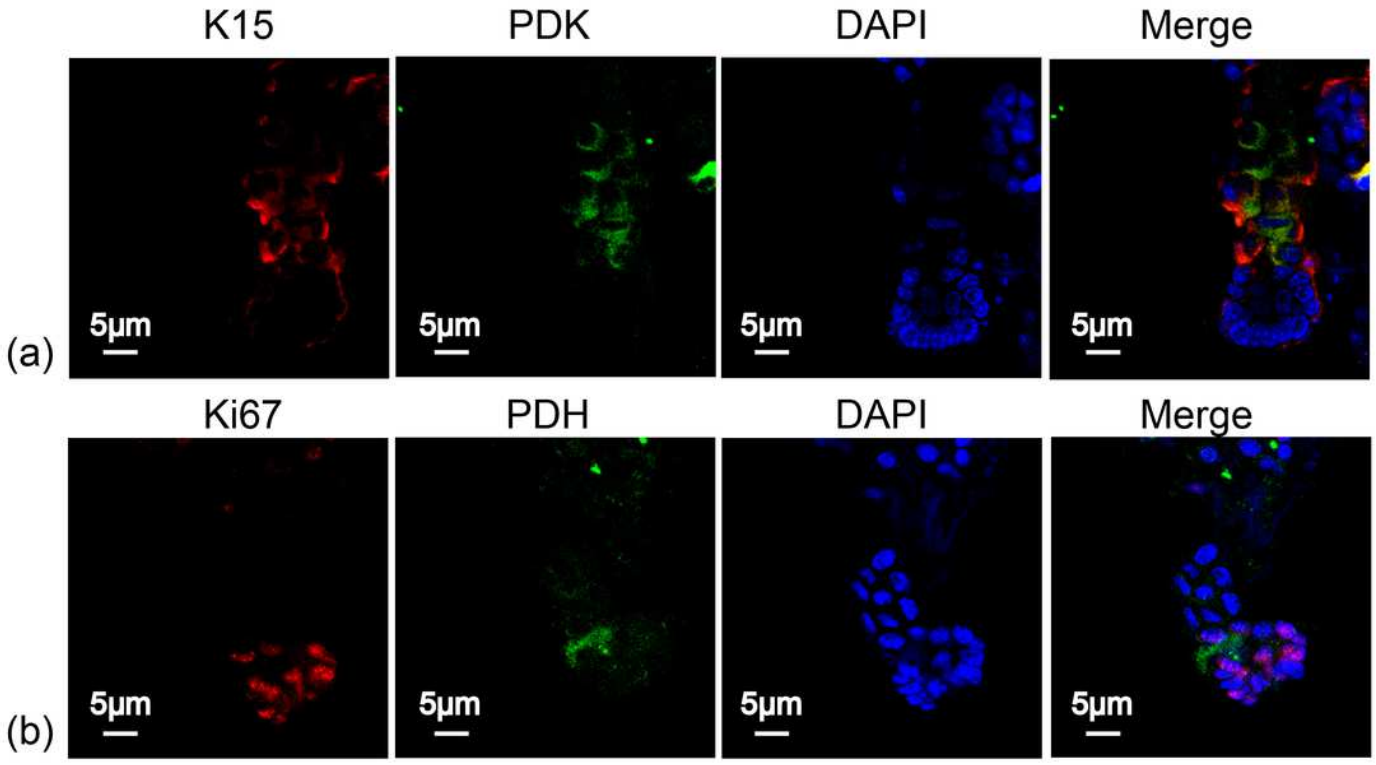

5

Inhibiting mitochondrial respiration retards hair regrowth.

Fig. 5. Inhibiting mitochondrial respiration retards hair regrowth. (a). Schematic diagram of our experimental approach. Mice were treated with Antimycin A intracutaneously on one side of the back skin, and DMSO on the contralateral side for 10 days. 200 hairs were plucked after three days of drug treatment (as shown in red arrow). Photos were taken at day 3, day 11 and day 19 after the start of treatment (as shown in blue arrow). (b). Photos of hair regrowth taken at day 3, 11, and 19 after treatment. At day 11, hair growth was observed in the DMSO treatment group (control group) while hairs failed to grow in the antimycin A treatment group, indicating that hair regeneration was held back in the antimycin A group. (c). It took much longer time in the antimycin A group (9.6 ± 0.9 days) in hair regrowth than that in the DMSO group (6.7±0.7 days) (**, $P < 0.01$). Data show a complication of 3 experiments (n=3 mice per group).